

Carleton Geology Department

Geology Comps Papers

Carleton College

Year 2004

The Steptoean Positive Isotopic Carbon
Excursion (SPICE) in siliciclastic facies
of the Upper Mississippi Valley:
Implications for mass extinction and sea
level change in the Upper Cambrian

David J. Auerbach
Carleton College,

The Steptoean Positive Isotopic Carbon Excursion (SPICE) in siliciclastic facies of the Upper Mississippi Valley: Implications for mass extinction and sea level change in the Upper Cambrian

**David J. Auerbach
Senior Integrative Exercise
March 10, 2004**

**Submitted in partial fulfillment of the requirements for a
Bachelor of Arts degree from Carleton College, Northfield, Minnesota**

Table of Contents

Abstract	iii
Introduction	1
Background	3
<i>Cambrian Laurentia</i>	3
<i>Stable carbon isotopes</i>	3
<i>Chemostratigraphy and biomerer</i>	5
<i>Lingulid brachiopods</i>	7
<i>Rare earth elements and paleoredox</i>	7
Methods	8
<i>Sample collection and preparation</i>	8
<i>Microscopy</i>	8
<i>Carbon isotopes</i>	8
<i>Elemental analyses</i>	14
Results	14
<i>Microscopy</i>	14
<i>Carbon isotopes</i>	16
<i>Major and trace elements</i>	18
<i>Rare-earth elements</i>	18
Discussion	18
<i>Diagenetic alteration</i>	20
<i>Paleoredox state</i>	23
<i>Cambrian carbon cycling and consequences for $\delta^{13}C$</i>	24
<i>A mechanism for extinction and the SPICE</i>	25
Conclusions	29
Acknowledgements	29
References	30
Appendix: Elemental data	35

The Steptoean Positive Isotopic Carbon Excursion (SPICE) in siliciclastic facies of the Upper Mississippi Valley: Implications for mass extinction and sea level change in the Upper Cambrian

David Auerbach
Carleton College
Senior Integrative Exercise
March 10, 2004

Advisors:

Clinton A. Cowan, Carleton College
Anthony C. Runkel, Minnesota Geological Survey
David Fox, University of Minnesota

Abstract

The Steptoean Positive Isotopic Carbon Excursion (SPICE) is a large ($\geq 4\%$ shift) positive carbon isotope ($\delta^{13}\text{C}$) excursion in the Upper Cambrian. The SPICE excursion begins at the base of the Pteroccephaliid Biomere, which is coeval with a mass extinction of shelf fauna and the initiation of the second of two major regressions in the Cambrian. It peaks at the Sauk II-Sauk III subsequence boundary, which corresponds to the height of the regression. New carbon isotope ($\delta^{13}\text{C}$) data from the carbonate phase of phosphatic lingulid brachiopods from Upper Cambrian nearshore siliciclastic facies in the Upper Mississippi Valley, USA show the presence of the SPICE. The shape and magnitude of the SPICE are consistent with results from whole-rock carbonate analyses. However, values in this study are consistently $\sim 6\%$ lower than whole-rock analyses due to fractionated carbon delivered to the nearshore by rivers. This study also reports a surge in concentrations of Fe as well as trace elements (Pb, As, Co, Cu, Ni, and Mo) known to be toxic to marine invertebrates just above the base of the Pteroccephaliid biomere. These perturbations were probably driven by the Sauk II-Sauk III regression, which exposed large areas of the Laurentian craton for the first time since inundation earlier in the Cambrian, allowing remobilization of Fe and toxic trace elements concentrated in sediments and soil. These elements were probably transported by rivers from exposed land to the epeiric sea, where concentrations would quickly have exceeded tolerances of most shelf fauna and caused widespread mortality. The influx of Fe could have stimulated primary productivity, resulting in increased burial of organic (^{12}C -enriched) carbon and the positive excursion of the SPICE.

Keywords: carbon isotopes, SPICE, biomere, mass extinction, phosphatic brachiopods, lingulids, Upper Cambrian, Sauk II-Sauk III boundary

Introduction

The Cambrian has been divided based on a number of faunal extinction events called biomes by Palmer (1965; 1981; 1984; 1998) (Fig. 1). The cause of these extinctions, in particular the Marjumiid-Pterocephaliid biome boundary, continues to be debated by paleontologists and sedimentologists, but recent hypotheses have argued for the incursion of an exotic water mass into a relatively warm epeiric sea (Saltzman et al., 1995; Perfetta et al., 1999). In particular, these models have focused on an influx of cold, anoxic water resulting from the overturn of a stratified ocean either separately or in conjunction with a rise in the thermocline and O₂ minimum zone from sea level change (Palmer, 1984; Perfetta et al., 1999). Previous work investigating various forms of this “cold water hypothesis” has included carbon isotope stratigraphy (Saltzman et al., 1995; Perfetta et al., 1999; Saltzman et al., 2000), rare earth element (REE) analysis (Thomas, 1993), and strontium isotope analysis (Saltzman et al., 1995; Montañez et al., 1996).

The Marjumiid-Pterocephaliid biome boundary (Marjuman-Steptoean stage boundary) is approximately coeval with the beginning of a major regression (Runkel et al., 1998) as well as a positive carbon isotope ($\delta^{13}\text{C}$) excursion of ~4‰ (Steptoean Positive Isotopic Carbon Excursion, or SPICE, event of Saltzman et al. (1998). This association of events suggests some significant disruption of the Cambrian hydrosphere-atmosphere-biosphere system. The stratigraphy of this interval in the Upper Mississippi Valley (UMV) has been well-studied by Runkel et al. (1998). Availability of abundant stratigraphic and biostratigraphic information makes the UMV an ideal location to further explore the mechanisms behind this series of events. This study presents new carbon isotope data from phosphatic inarticulate brachiopods which demonstrate for the first

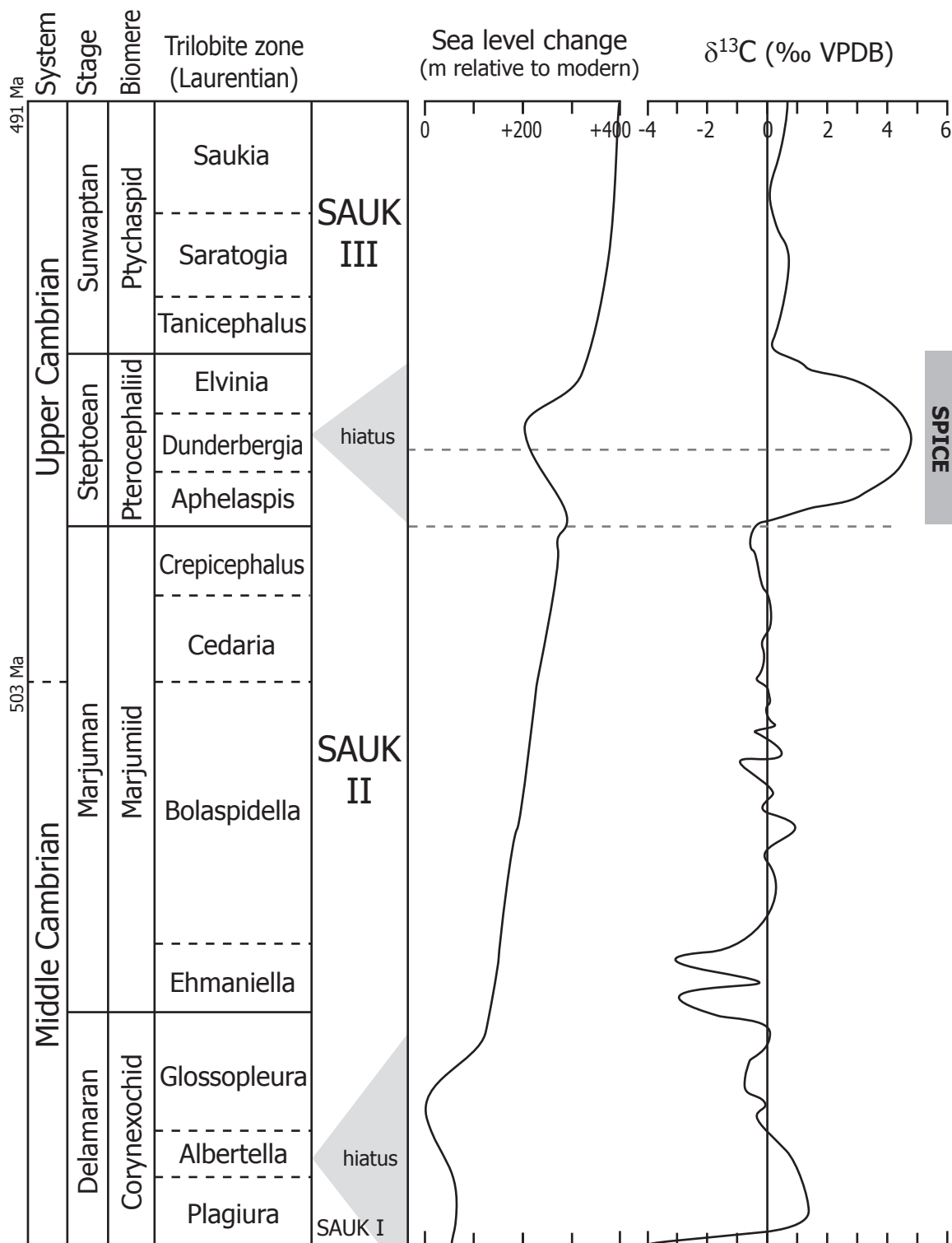


Figure 1. Representative sea level (modified from Dott and Batten (1981) and Runkel et al. (1998)) and carbon isotope curve (generalized from Saltzman et al. (1998), Montañez et al. (2000) and Saltzman et al. (2000)) shown against stratigraphic nomenclature for the Middle and Upper Cambrian (modified from Palmer (1981, 1998)). Dates after Saltzman et al. (in press).

time the presence of the SPICE in siliciclastic facies, accompanied by a perturbation of background elemental levels.

Background

Cambrian Laurentia

Sea level change during the Cambrian may be summarized by an overall trend of transgression (Dott and Batten, 1981) interrupted by two significant regressions. These regressions define the Sauk I-II and Sauk II-Sauk III subsequence boundaries (Palmer, 1981). By the Late Cambrian, large portions of the Laurentian craton were inundated, creating an epeiric sea (Dott and Batten, 1981). The sedimentary regime has been divided into three general facies belts (Fig. 2): the inner detrital belt and middle carbonate belt on the continental shelf and the outer detrital belt located off the edge of the craton (Palmer, 1971). The shelf edge was ringed by a carbonate bank-like structure, analogous (albeit on a much larger scale) to the modern Bahama Bank. This structure probably resulted from carbonates tracking transgressing sea level through the Cambrian.

Stable carbon isotopes

Carbon has two stable isotopes, ^{13}C and ^{12}C (Rollinson, 1993). The ratio of ^{13}C to ^{12}C can be determined by reacting carbonate material with an acid to release CO_2 gas that is measured using a mass spectrometer. Carbon isotope results are reported in standard delta (δ) notation:

$$\delta^{13}\text{C} = \left(\frac{R}{R_{std}} - 1 \right) \times 1000\text{‰},$$

Late Cambrian paleogeography of Laurentia

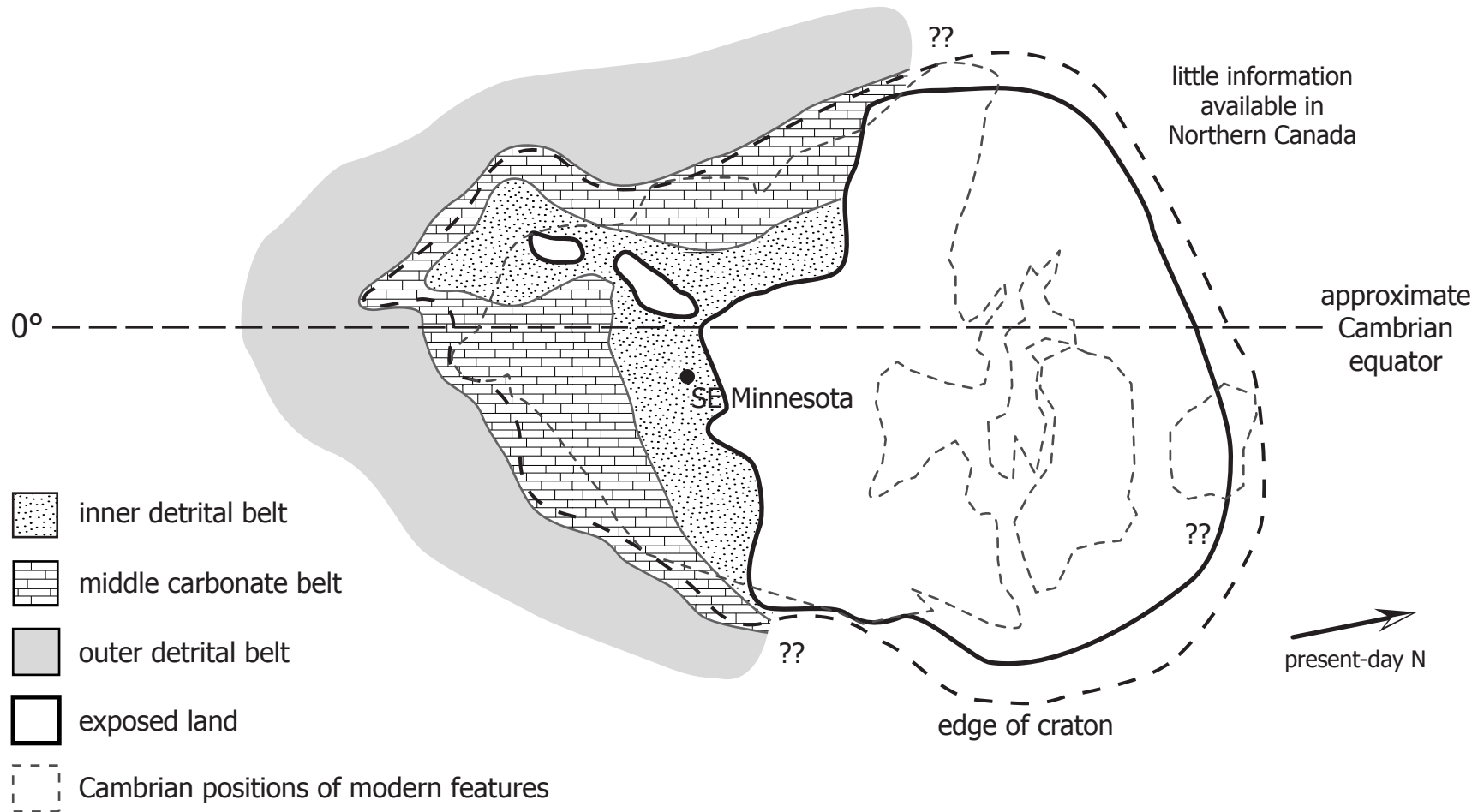


Figure 2. Interpretive Cambrian paleogeography (adapted from Dott and Batten, 1981) with facies belts (after Palmer, 1971).

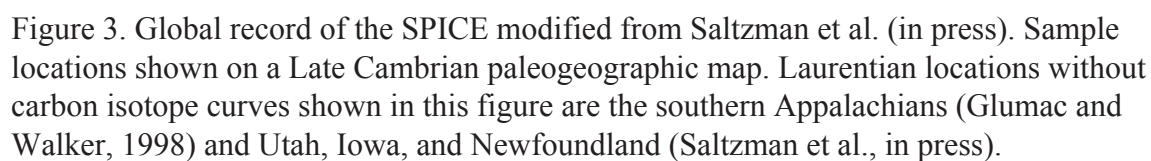
where R is the measured ratio of ^{13}C to ^{12}C and R_{std} is the ratio in a reference standard.

The common reference standard is belemnite material from the PeeDee formation in South Carolina, which is used because it is close to the average value for marine limestone.

Because ^{13}C and ^{12}C have different atomic masses, they are subject to fractionation. Certain processes such as evaporative diffusion and biological uptake preferentially utilize lighter ^{12}C . This depletes certain reservoirs of ^{13}C and enriches others, resulting in a corresponding decrease or increase of $\delta^{13}\text{C}$ values.

Chemostratigraphy and biomes

Cambrian biomere boundaries are thought to be global events (Fig. 3) defined by the extinction of numerous trilobite genera and other members of shelf communities (Palmer, 1965, 1984). They do not correlate well with lithologic changes, nor have they been successfully connected with impact events (Palmer, 1984). The Marjumiid-Pterocephaliid biomere boundary (Fig. 1) has been particularly well-studied because of its association with major sea level changes and the SPICE. The conspicuous carbon isotope stratigraphy of this interval has been recognized in carbonate rocks globally. Laurentian locations include Colorado (Brasier, 1993), Nevada, Utah, (Saltzman et al., 1998), South Dakota (Perfetta et al., 1999), Iowa, Newfoundland, (Saltzman et al., 2004), Missouri (Cowan et al., 2003), and Tennessee (Glumac and Walker, 1998). However, traditional whole-rock isotopic analysis has been limited to carbonates and cannot be applied to the siliciclastic facies of the inner detrital belt.



Lingulid brachiopods

The members of class *Lingulata* (phylum *Brachiopoda*) are sessile bivalvate lophophorates (Stearn and Carroll, 1989). They secrete organophosphatic shells with alternating layers of apatite (calcium phosphate) and chitin (Williams et al., 1994). Modern lingulid shells have been found to be precipitated in oxygen isotopic equilibrium with seawater, independent of any biologic fractionation (vital effect) (Rodland et al., 2003). Carbonate ions (CO_3^{-2}) can substitute for phosphate (PO_4^{-3}) during biogenic precipitation of apatite. This carbonate phase has been found to yield reliable stable isotope information. The carbonate phase contains both oxygen and carbon, permitting the possibility that lingulids shells are also precipitated in carbon isotopic equilibrium with seawater. This is further suggested by a lack of evidence for a vital effect in calcitic brachiopods (Lee and Wan, 2000).

Lingulids appear in rocks through the entire Phanerozoic, and their morphology and physiology have undergone little apparent evolutionary change during that time (Lécuyer et al., 1996). Modern lingulids excavate shallow burrows, but this sessile lifestyle did not develop until the Ordovician (Stearn and Carroll, 1989); Cambrian lingulids are postulated to have been motile burrowers that lived in shallow sediments.

Rare earth elements and paleoredox

Skeletal material of marine organisms (e.g. apatite) acquires a rare earth element (REE) signature at the sediment-water interface after the death of an organism (Wright et al., 1987). The length of time that skeletal material remains at the sediment-water interface controls REE concentrations (Wright et al., 1987), but the shape of the REE pattern (Fig.

4) acquired from seawater reflects the aeolian and fluvial sources contributing to a body of seawater (Elderfield et al., 1990). Modern phosphatic brachiopod shells have "hat-shaped" REE patterns whereas diagenetically altered shells have "bell-shaped" patterns (Lécuyer et al., 1998) (Fig. 4).

Significant paleoceanographic events, such as a rise of the O₂ minimum zone or destratification, should change the redox state of marine waters. Elemental systematics can offer an indication of redox state. Most rare earth elements (REE) are trivalent (3+) and have only one oxidation state, the exceptions being cerium (Ce³⁺, Ce⁴⁺) and europium (Eu²⁺, Eu³⁺). When Ce is oxidized to Ce⁴⁺, it is quickly removed from the water column by precipitation as a component of organic and metallic oxide complexes (Laenen et al., 1997), although the organic complexing was probably not well-developed in the early Paleozoic (Picard et al., 2002). Reduced Ce³⁺, however, is more likely to remain dissolved in seawater and be absorbed by skeletal material. Wright et al. (1987) were the first to suggest that this fractionation of Ce in seawater may provide a useful indicator of paleoredox state in marine waters. The lack of measurable variation in Ce fractionation across phosphatic brachiopod species also offers the possibility that Ce may be a robust paleoredox indicator. The magnitude of the Ce anomaly relative to a normalized REE profile is expressed as

$$\Omega_{Ce} = \log\left(\frac{Ce}{Ce^*}\right),$$

where Ce is the measured concentration and Ce^{*} is the interpolated value between lanthanum (La) and neodymium (Nd), the neighboring values on a typical REE plot. $\Omega_{Ce} < 0.1$, the result of a negative Ce anomaly on an REE plot, is taken to indicate oxidizing

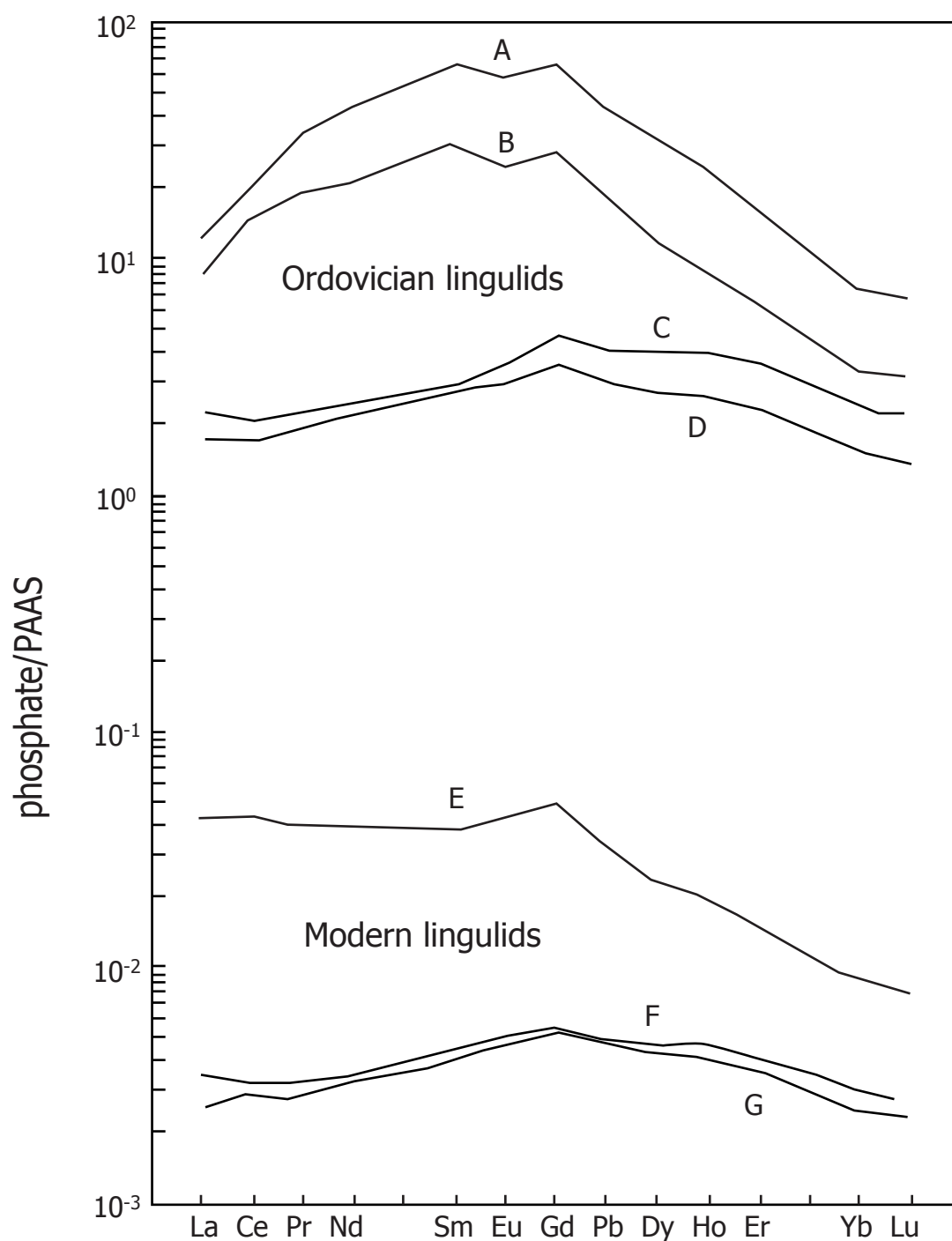


Figure 4. Characteristic REE patterns modified from Lécuyer et al. (1998). Analyses of Paleozoic shell material yield patterns with enriched two to three orders of magnitude compared to modern shell material. Analyses from modern lingulids (E, F, G) have hat-shaped REE patterns, although the E shows LREE enrichment (see Discussion). Analyses A and B from Ordovician lingulids have bell-shaped patterns associated with diagenetic alteration, but, C and D have unaltered hat-shaped patterns similar to modern lingulids. It appears that REE patterns can be preserved independent of overall REE concentrations.

conditions (Wright et al., 1987). There is some ambiguity if $\Omega_{Ce} > 0.1$, the result of a positive anomaly on an REE plot, indicates reducing conditions (Laenen et al., 1997).

Methods

Sample collection and preparation

Samples were collected from lingulid-rich lag deposits (Fig. 5) at an outcrop in Hudson, WI, and in two cores taken by the Aquifer Thermal Energy Storage project on the St. Paul campus of the University of Minnesota. The samples span a stratigraphic interval from the upper Mt. Simon Formation to the lower Franconia Formation (Fig. 6). Fossil brachiopod valves were isolated by hand from rock samples under a binocular microscope. Shells were washed in deionized water and cleaned using an ultrasonic cleaner at Carleton College to remove residual cement and detrital grains. Securely cemented grains were removed using a dental drill with a diamond bit at the University of Minnesota. Cleaned shells were crushed with an agate mortar and pestle.

Microscopy

A lingulid valve from sample 864'1" (core BC-1) was cut perpendicular and parallel to the growth axis and examined using a JEOL JSM-5300 scanning electron microscope (SEM) at Carleton College to assess possible alteration.

Carbon isotopes

Sample powders were bathed in 2-3% sodium hypochlorite for 24 hours to remove any organic matter, after which they were rinsed five times with ultrapure water. They were

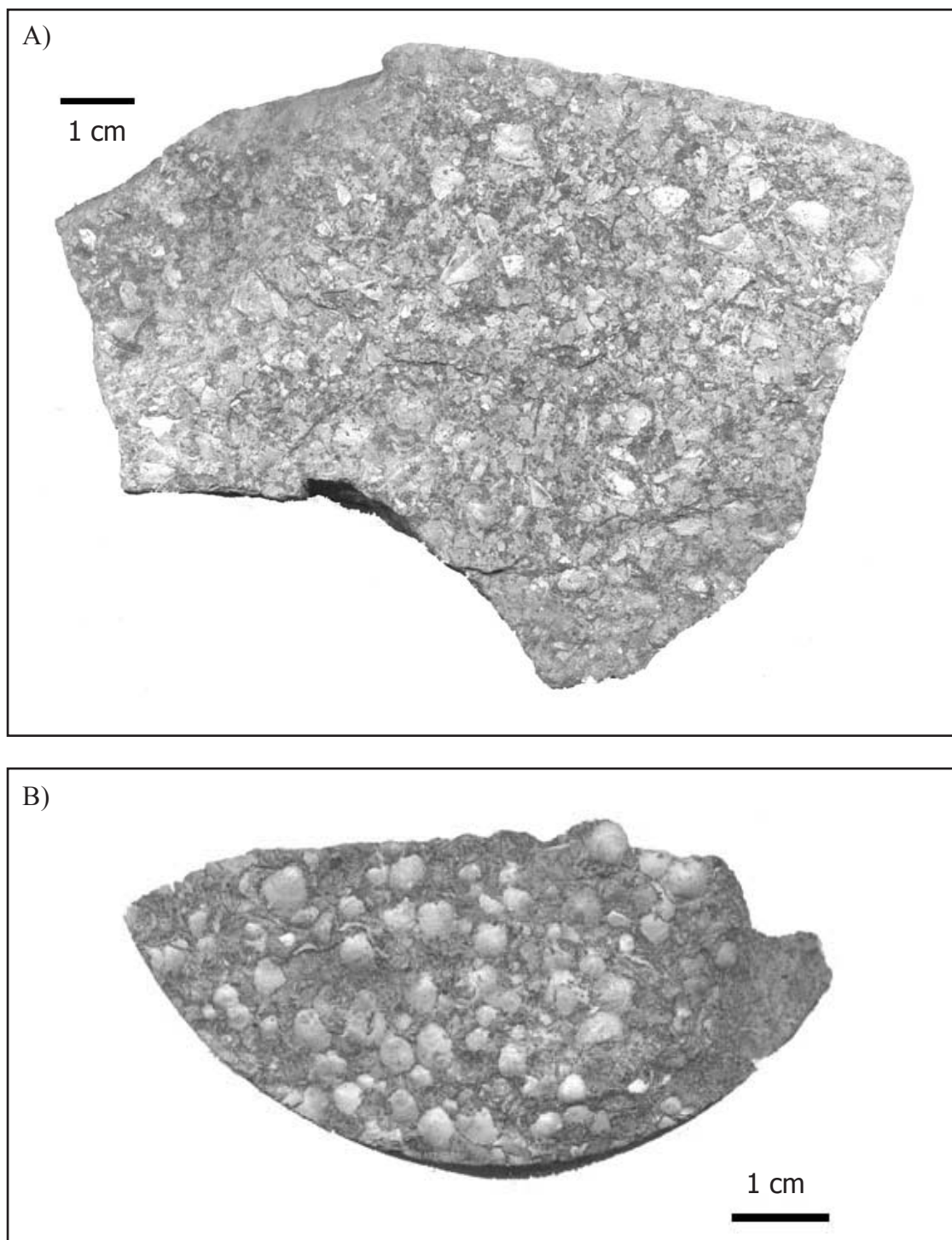


Figure 5. Storm lags of lingulid brachiopod shells from A) outcrop and B) core. Growth rings and an apparently primary sheen are still visible (see text for discussion).

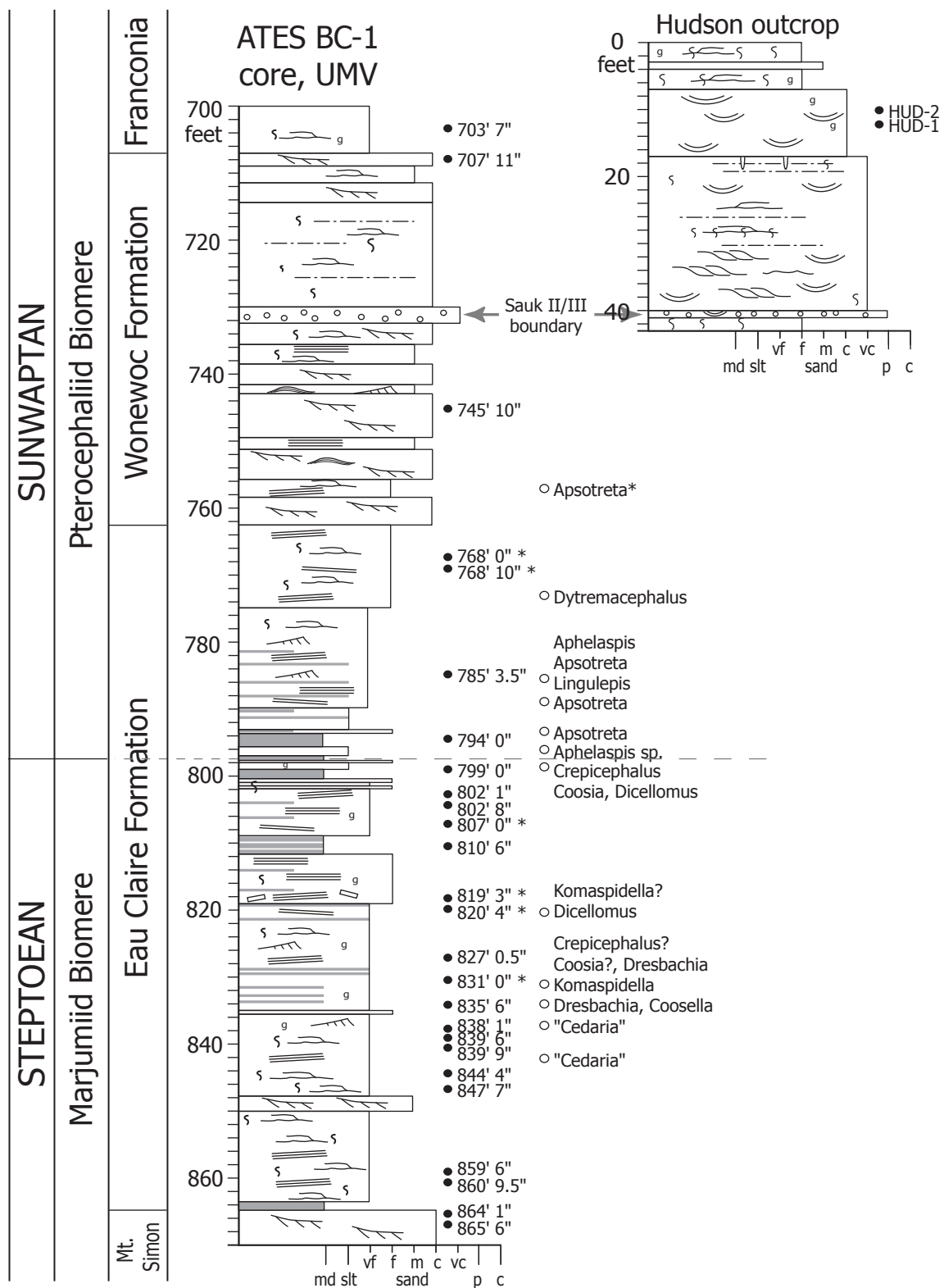


Figure 6. Stratigraphic column of BC-1 core and Hudson outcrop showing sample locations. Columns and trilobite biostratigraphy from Runkel et al. (1998). Sections correlated based on the quartz pebble bed that probably represents the peak of the Sauk II-III regression (Runkel et al., 1998). See Fig. 7 for key.

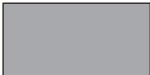
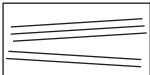





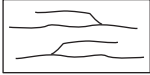

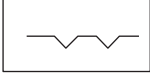

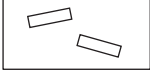

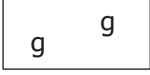

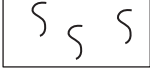
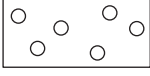

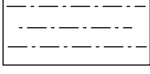


	shale		low-angle, hummocky to horizontal stratification
	horizontal shale laminations or beds		lateral accretion bedding
	cross-strata (uncertain geometry)		shale laminae/drapes and lenticles
	trough cross-strata		disrupted shale laminae and beds
	swaley cross-strata		cracks
	hummocky cross-strata		intraclasts
	ripple cross-strata		glaucinite
	dune bedforms		burrows or bioturbated fabric
	pebbles and granules		large vertical burrows, e.g. Skolithos (>1cm diam)
	silt/shale matrix in sandstone		Aphelaspis trilobites (from Runkel et al., 1998)
* from companion core AC-1			810' 6" sample position/tag, this study

Figure 7. Key for stratigraphic columns in this study (adapted from Runkel et al., 1998)

then treated with 1M acetic acid with a calcium acetate buffer for 24 hours. Samples were rinsed with ultrapure water five more times and vacuum freeze-dried overnight to remove any remaining water. The resultant material was reacted with phosphoric acid to liberate CO₂ in a Finnigan “Kiel” Carbonate III preparation device coupled to a Finnigan MAT 252 mass spectrometer, which was used to measure the isotopic composition of the CO₂. Reproducibility was maintained at better than $\pm 0.1\%$ by repeated runs of carbonate standards NBS-18 and NBS-19. $\delta^{13}\text{C}$ is reported relative to the Vienna PeeDee Belemnite (VPDB) standard.

Elemental analyses

Sample powders were dissolved in HNO₃⁻ and heated at 50°C for 4 hours. The samples were diluted with deionized water to experimentally determined concentrations. These solutions were analyzed on a ThermoElemental PQ ExCell ICP-MS instrument at the University of Minnesota for major, trace, and rare-earth element concentrations. Calibration was based on NIST traceable standards which were also checked against NIST water trace element standard 1640. Major elements analysis was also performed with a Dionex ICS-2000 ion chromatograph to verify precision of ICP-MS results.

Results

Microscopy

SEM examination shows the preservation of fine microstructures (Fig. 8). The shells have a dense outer “primary” zone and an inner “secondary” zone made up of alternating <10 μm thick layers of chitinous laminae and 70-80 μm long baculate rods of

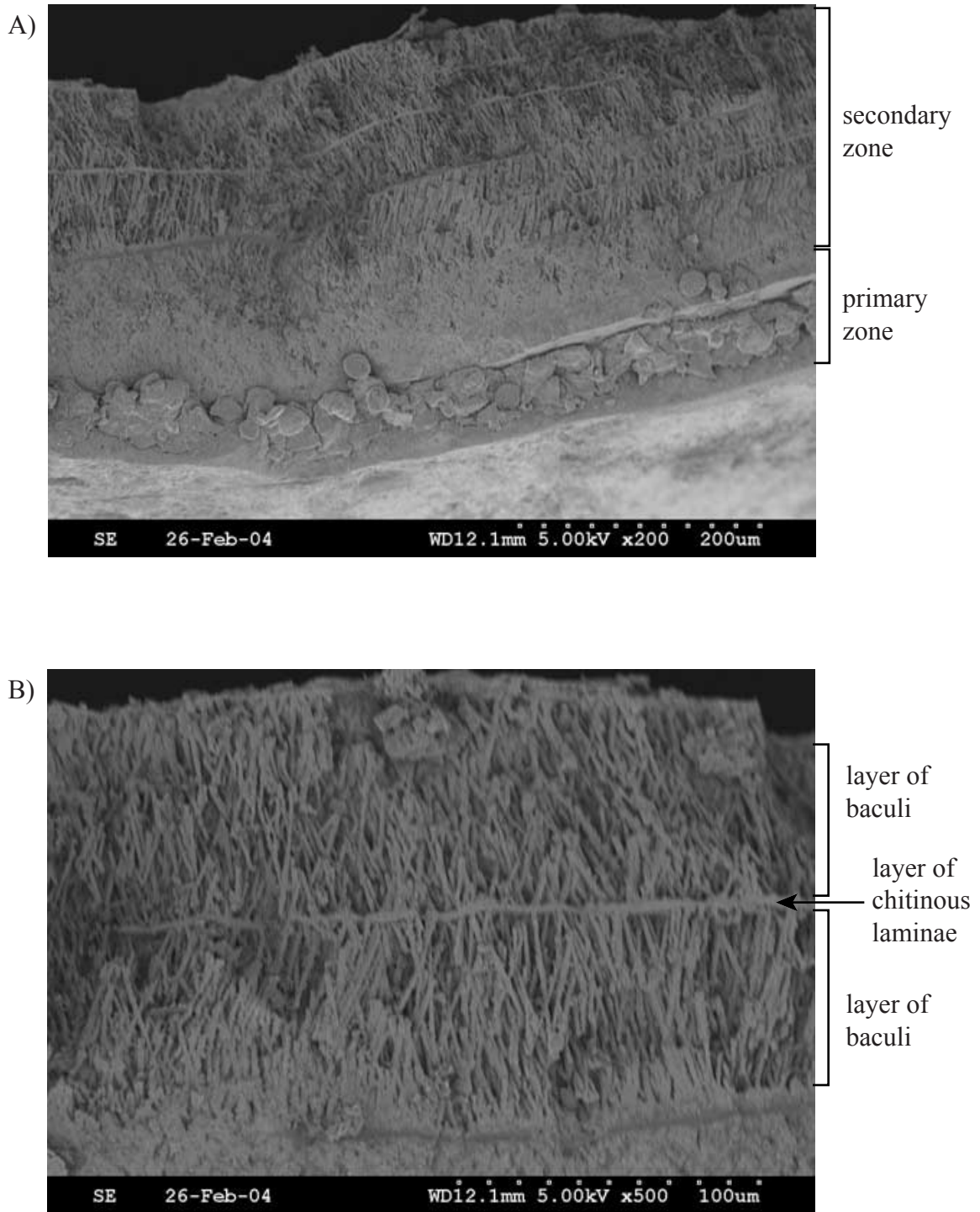


Figure 8. SEM images of a brachiopod valve cut perpendicular to growth rings. A) Primary and secondary zones. B) Secondary layer showing alternating layers of baculate apatite rods and chitinous lamellae.

apatite. Identical structures are present in upper Paleozoic lingulids (Williams et al., 1994) and are similar to structures found in unaltered modern specimens from groups such as *Glottida* (Williams and Cusack, 1999).

Carbon isotopes

Carbon isotope ($\delta^{13}\text{C}$) values from lingulid valves (Fig. 9, Table 1) vary little from around -6‰ through the stratigraphic section (Fig. 6) until the Marjumiid-Pterocephaliid biomere boundary. After the boundary (~22 m) values rapidly increase to around -1.5‰ and remain high until ~49 m, where values decrease to end slightly below -3‰. This excursion is of similar shape, magnitude, and biostratigraphic position to the SPICE (Fig. 9). In constructing the isotope curve (Fig. 9), samples not from core BC-1 were correlated using the Sauk II-III boundary as datum and assuming equal thicknesses.

Source	Sample	$\delta^{13}\text{C}$ (‰ VPDB)	Fe	Co	Ni	As	Mo	Pb	Cu	Ω_{Ce}
BC-1 (core)	703'7"	-2.442	7833.00	77.63	65.23	61.30	3.38	55.83	301.00	0.35
BC-1	707'11"	-1.338	8132.00	203.80	202.30	135.30	6.44	184.40	445.50	0.33
BC-1	745'10"	-1.618	5108.50	78.41	169.60	56.05	5.96	136.60	181.50	0.30
BC-1	794'0"	-4.206								
BC-1	799'0"	-6.579								
BC-1	802'1"	-7.211	3299.00	5.19	19.96	14.21	2.23	8.01	109.20	0.29
BC-1	847'7"	-6.160								
BC-1	859'6"	-6.155	6446.00	1.36	9.18	18.16	1.22	26.35	79.46	0.44
BC-1	860'9.5"	-3.153	3988.50	0.75	10.57	17.37	2.05	31.13	100.28	0.33
BC-1	864'1"	-6.254	5921.00	5.52	20.56	24.55	3.21	66.98	466.60	0.41
BC-1	865'6"	-5.666	6183.50	0.67	6.98	19.56	1.09	36.79	257.50	0.28
AC-1 (core)	736'0"	-1.883	7763.50	333.80	247.00	166.80	9.85	175.30	257.20	0.34
AC-1	736'10"	-1.820	11335.00	382.40	227.80	171.20	11.70	189.30	510.10	0.33
Hudson (outcrop)	1	-2.338								
Hudson	2	-3.132	8941.00	2.19	22.68	24.66	1.97	160.60	297.70	0.37

Table 1. Carbon isotope results, selected major and trace element concentrations, and Ω_{Ce} for the stratigraphic interval described in Fig. 6. All elemental concentrations in ppm.

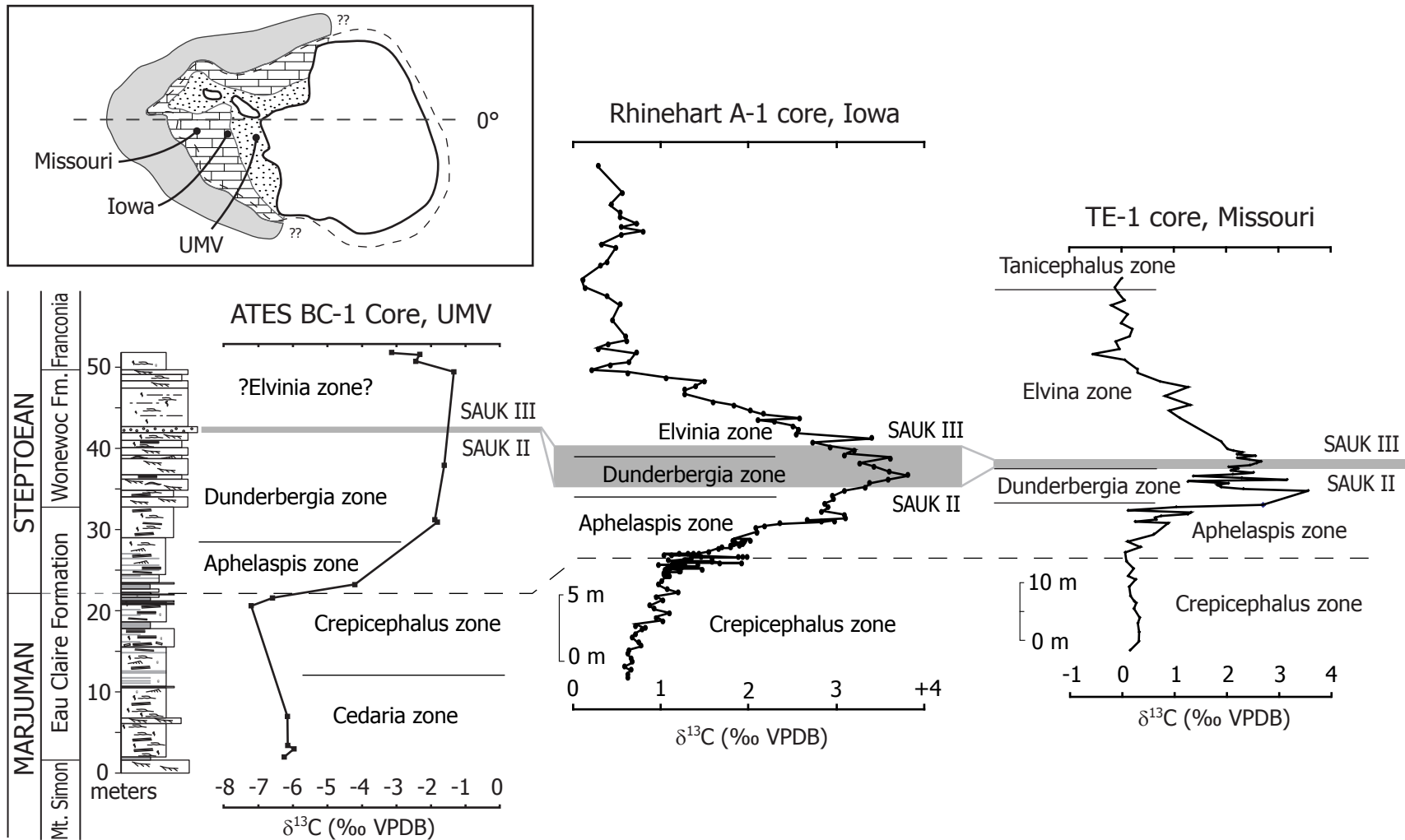


Figure 9. Carbon isotope data of this study correlate well with the shape and timing of with other occurrences of the SPICE. Locations of sample sites in Laurentian paleogeography shown at top left (see Fig. 2 for details) Rhinehart A-1 curve after Saltzman et al. (in press), TE-1 curve from Cowan et al (2003).

Major & trace elements

Concentrations of selected major and trace elements (Fig. 10, Table 1) show rapid increases of six to ten fold after the Marjumiid-Pterocephaliid biomere boundary and then either decrease (Cu, As, Co) or flatten out (Fe, Pb, Ni, Mo) above 31 m. Most concentrations decrease sharply above ~49 m. Complete elemental data is available in Appendix 1 (Fig. A1).

Rare earth elements

Rare earth element data shows hat-shaped patterns with enrichment of the light rare earth elements (LREE), lanthanum through europium, in all samples (Fig. 11). These patterns are punctuated by a positive Ce anomaly with Ω_{Ce} ranging from 0.28 to 0.44 (Fig. 12, Table 1).

Discussion

The nearshore environment is subject to substantial variations in freshwater input levels over short time scales (Lécuyer et al., 1996). This has caused concern about the reliability of stable isotope and geochemical data from samples from nearshore environments (e.g. Lécuyer et al., 1996; Picard et al., 2002). However, stable isotope evidence from modern oysters in mixed marine-freshwater environments indicates that shell growth is significantly diminished during periods of unusually low salinity from freshwater flooding (Sarkar et al., 2003). It is likely that lingulids living in the nearshore had similar sensitivities and thus primarily recorded stable isotope and geochemical

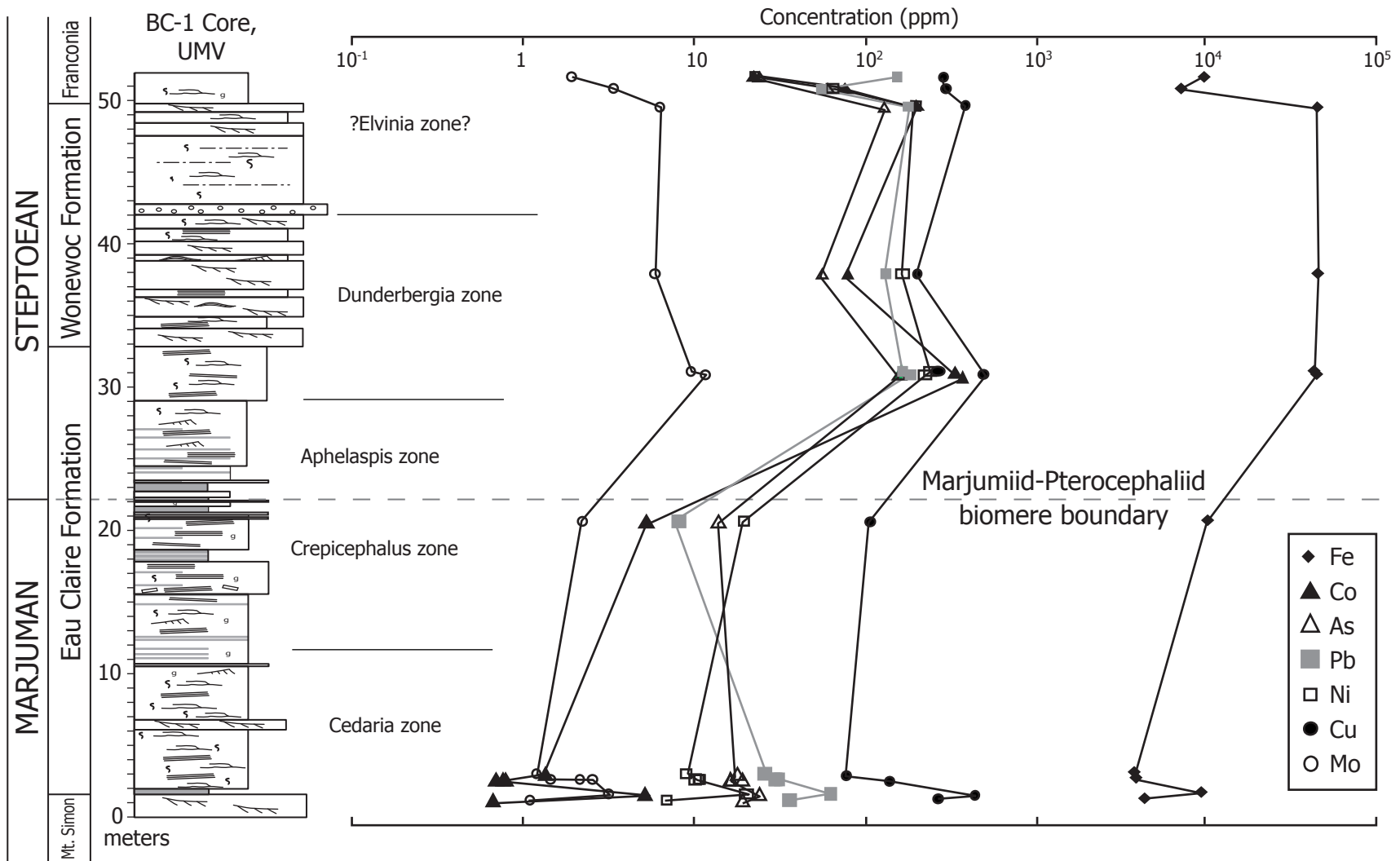


Figure 10. Selected major and trace element concentrations show increases by a factor of approximately 6 to 10 after the Marjumiid-Pterocephaliid biomere boundary, but do not continue to increase all the way to the Sauk II-Sauk III boundary.

information of the marine conditions that favored their growth. Because entire valves were crushed for analysis, information from such conditions will dominate the results.

A second consideration is brachiopods in this study were collected from lag deposits. Because stable isotope and geochemical analyses required multiple brachiopod valves, the results of these analyses are effectively spatial and time averages. The spatial and temporal extent of this averaging effect is limited by sequence and biostratigraphic information but is difficult to determine with precision.

Diagenetic alteration

Although the lingulid shells in hand sample still show growth rings and an apparently primary sheen (Fig. 5), it is important to rigorously establish the diagenetic integrity of the phosphatic shells because of the early Paleozoic age of the samples in this study. This study employs both microscopic examination of morphological details and chemical evaluation of shell material. The delicate baculate apatite growth structures seen under SEM examination (Fig. 8) would not have been preserved if they had been strongly recrystallized during diagenesis. The spaces between the baculi were filled with proteins called glycosaminoglycans during the life of the brachiopod that presumably decayed post-mortem (Williams and Cusack, 1999).

Independent of the Ce anomaly, the shape of the REE patterns in Figure 11 show close similarity to REE patterns of modern LREE-enriched nearshore lingulids from New Caledonia reported by Lécuyer et al. (1998) (see pattern E in Fig. 4). LREE enrichment may be explained by fluvial input from LREE-enriched volcanic or plutonic source regions (Lécuyer et al., 1998; Picard et al., 2002). In the case of Lécuyer et al. (1998) the

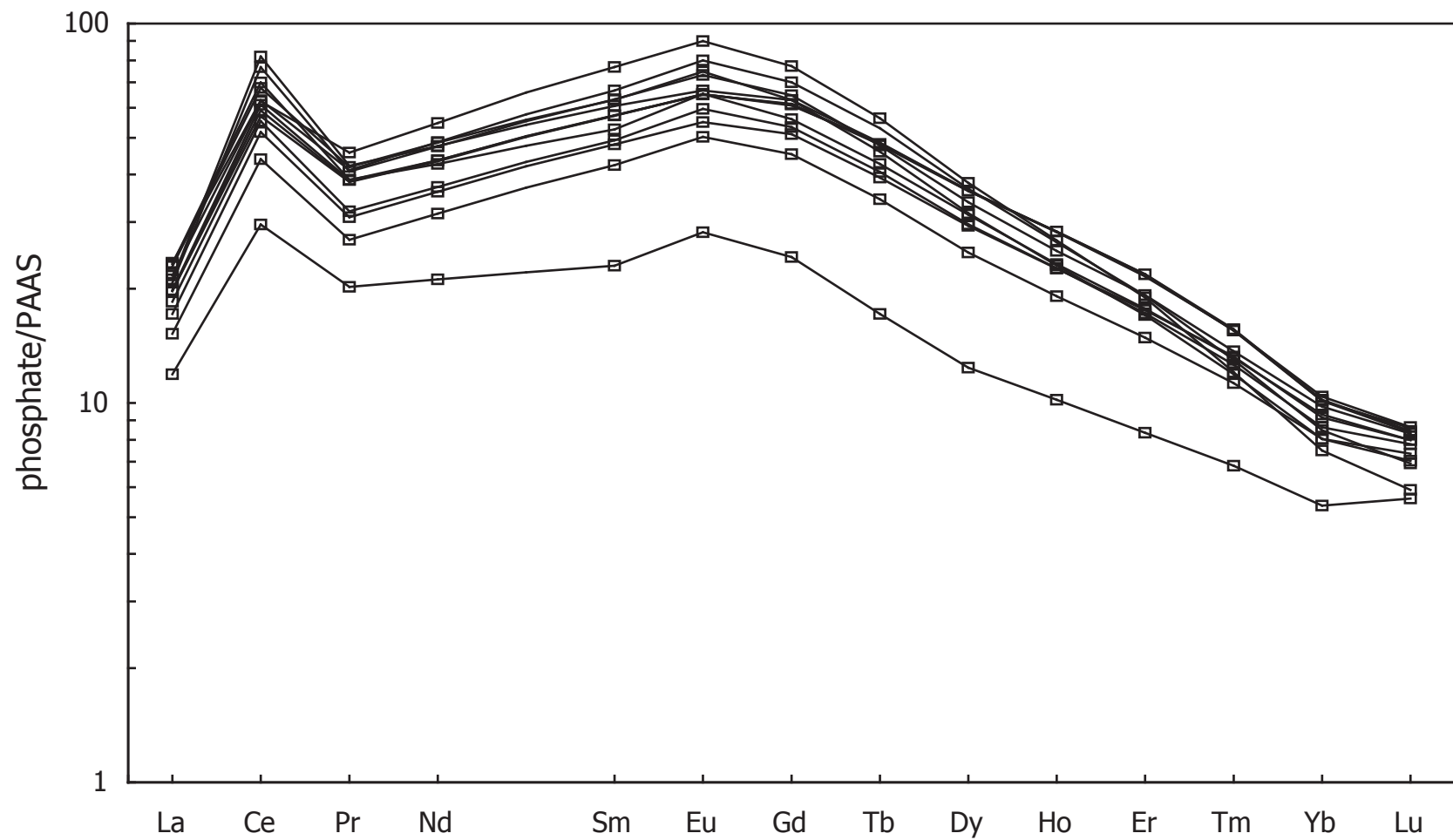


Figure 11. REE concentrations in phosphatic brachiopod shells, normalized to the Post-Archaeon average Australian Sedimentary rock (PAAS) standard (McLennan, 1989). Patterns are hat-shaped (see text for discussion), indicating that the samples have not been diagenetically altered. LREE enrichment is also visible. These patterns are interrupted by a positive cerium anomaly.

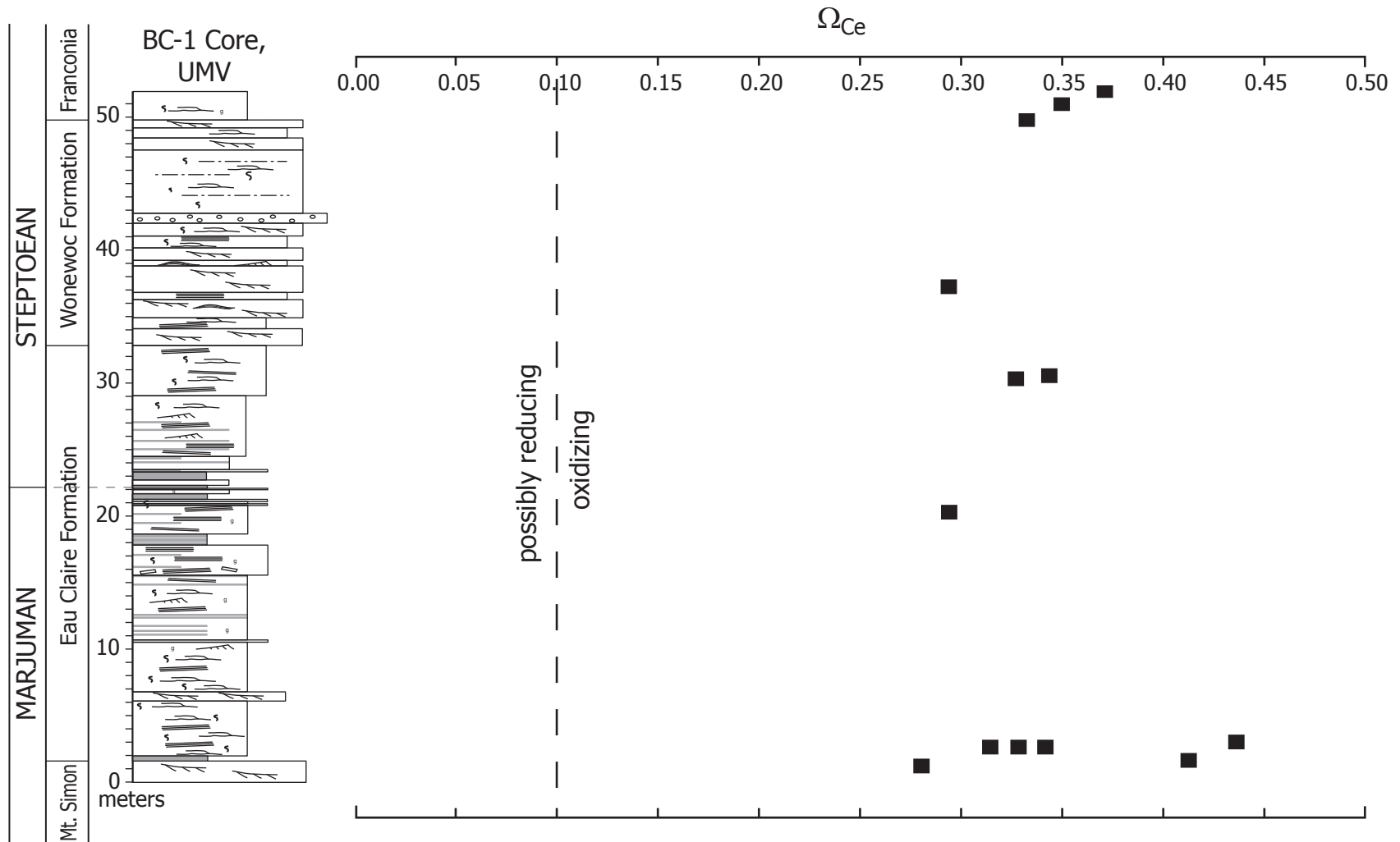


Figure 12. Ω_{Ce} is between 0.25 and 0.45 through the stratigraphic interval. Equation used in calculation is $\Omega_{Ce} = \log ({}^{2/3}La_n + {}^{1/3}Nd_n)$ from Elderfield et al. (1990). Division in redox state after Wright et al. (1987). See text for significance of $\Omega_{Ce} > 0.1$.

LREE enrichment may be due to the unusually high concentration of ultramafic rocks on New Caledonia (Latham, 1975). The overall increase in concentrations relative to modern lingulids is about three orders of magnitude, which is also similar to other early Paleozoic samples analyzed by Lécuyer et al. (1998). During diagenetic alteration the middle rare earth elements (MREE), neodymium through holmium, are typically enriched because the MREE have ionic radii similar to Ca and P and substitute into crystal structures containing these elements (e.g. apatite) most easily; uptake of LREE by shell material is exponentially less likely (Reynard et al., 1999). However, no observable MREE enrichment relative of the hat-shaped patterns is observed; there in fact may be slight europium (Eu) depletion.

Both qualitative and quantitative assessments indicate the brachiopod valves analyzed in this study are diagenetically unaltered and have a good chance of preserving geochemical information from the Cambrian. Additional *prima facie* evidence for the quality of the brachiopod shells is the simple fact that they exhibit the SPICE. The SPICE is a conspicuous, widespread phenomenon in the chemostratigraphic record (Fig. 3) that should not be preserved in rocks altered by marine diagenesis.

Paleoredox state

The redox state of the nearshore apparently did not change significantly during the SPICE, as the Ce anomaly changes little across the stratigraphic interval of this study (Fig. 12). Ω_{Ce} values are all above 0.1, suggesting that conditions in shallow nearshore sediments (where the lingulids lived) were not oxidizing. However, lingulids are known to live in environments above fair-weather wave base (FWWB), as facies information

indicates (Fig. 4). Marine waters and shallow sediments above FWB are constantly mixed and oxygenated by wave agitation (Walker and Plint, 1992; Lécuyer et al., 2004). Terrigenous influx would almost certainly be oxidized as well (Picard et al., 2002). Laenen et al. (1997) have suggested that positive Ce anomalies may also be caused by the release of reduced pore water from deeper in the sediment column. Such a pore water flux could have occurred shortly after burial, as sandstones are highly porous. Regardless, the Ce anomaly does not appear to offer useful information about redox state of the nearshore in the Late Cambrian.

Cambrian carbon cycling and consequences for $\delta^{13}\text{C}$

The excursion in the carbon isotope data (Fig. 9) occupies a similar stratigraphic interval and is of similar magnitude to the SPICE event previously documented by numerous workers (e.g. Saltzman et al., 1998; Perfetta et al., 1999; Saltzman et al., 2000; Saltzman et al., 2003). However, the measured $\delta^{13}\text{C}$ curve (baseline and excursion) is shifted approximately 6‰ negative in comparison to other reported values from micrites of the middle carbonate belt. This significant difference is most likely due to the fact that lingulid habitats are closer to the shore than the middle carbonate belt (Fig. 2). $\delta^{13}\text{C}$ concentrations of dissolved carbon in modern rivers range from about -6‰ to -16‰ (Chao et al., 1996; Telmer and Veizer, 1999; Barth et al., 2003), depending on the soil composition and type of bedrock in the river's drainage region. Soil carbon is largely derived from terrestrial biota, which in the Cambrian would have been communities of bacteria, algae, and lichens (Dott, 2003). Modern lichens found in Australia have $\delta^{13}\text{C}$ values ranging from -22‰ to -27‰ (Batts et al., 2004). If this range of values was typical

for terrestrial microbial communities in the Cambrian, and lingulids precipitate their shells in isotopic equilibrium with seawater (without any vital effect), we can create a simple model to predict the contribution of fluvial carbon to nearshore $\delta^{13}\text{C}$ values (Fig. 13).

Changes in carbon isotope ratios during SPICE would have been reflected in both riverine and marine waters because the atmosphere and oceans equilibrate on short time scales (<50 years) (Koch et al., 1992). However, the $\delta^{13}\text{C}$ values of riverine carbon are shifted more negative than oceanic values by several fractionation steps (Fig. 13). Nearshore waters are frequently a mixture of marine and riverine water, and mixing results in an intermediate of these two isotopic signatures. The model presented here postulates that the percentage of riverine input to the nearshore environment where the lingulids used in this study lived was from 20% to 40%. Such a range is reasonable, as brackish environments such as these are known to be inhabited by modern lingulids (Lécuyer et al., 1996) and bivalvate mollusks (Halley and Roulier, 1999; Sarkar et al., 2003), which now occupy many of the ecological niches of Paleozoic brachiopods (Stearn and Carroll, 1989). One can conclude that while marine waters contributed the majority of the carbon to these environments, the strongly negative riverine signature still had a significant impact on the carbon isotopic value nearshore.

A mechanism for extinction and the SPICE

Previous workers (e.g. Palmer, 1981; Saltzman et al., 2000) have suggested the Marjumiid-Pterocephaliid extinction and perhaps the SPICE were driven by oceanographic changes in oxygen levels and temperature. This is not a convincing argument in light of

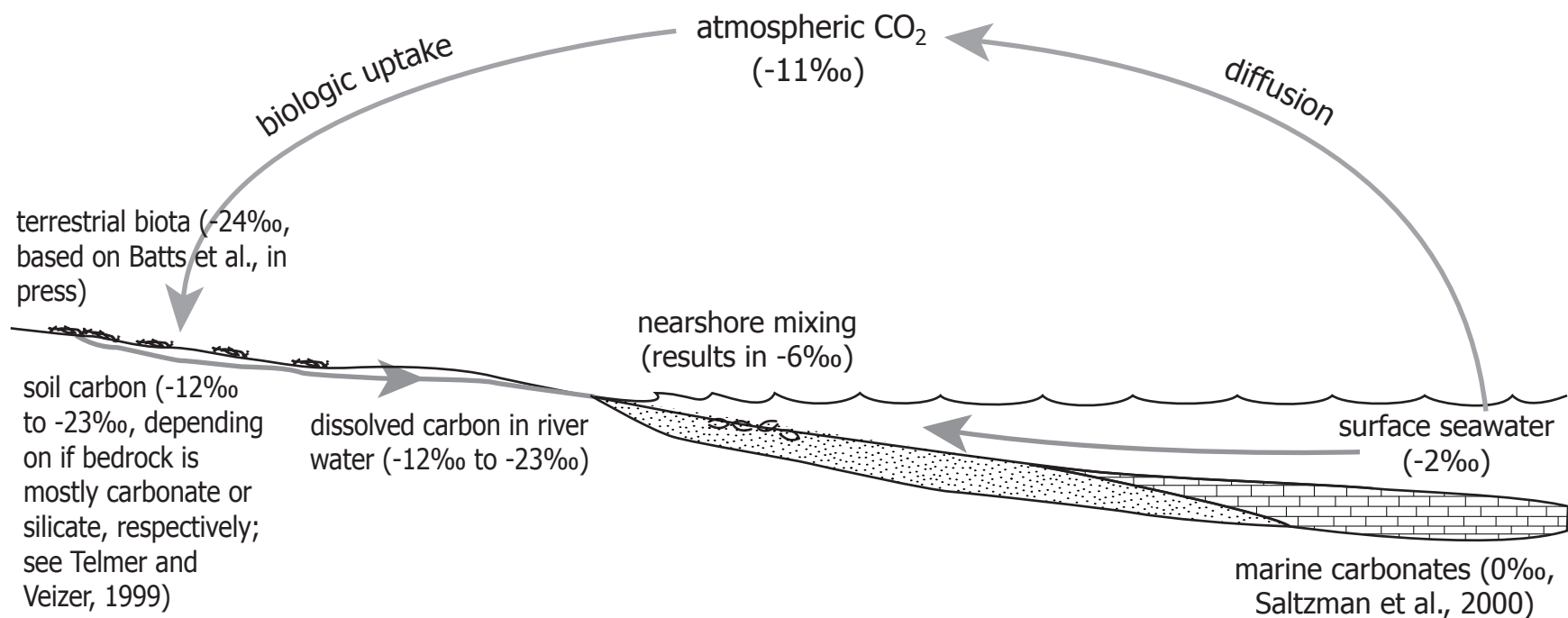


Figure 13. Schematic Cambrian carbon transport scheme showing hypothetical $\delta^{13}\text{C}$ values of reservoirs. Nearshore $\delta^{13}\text{C}$ values are the result of mixing of strongly negative carbon delivered by rivers and only slightly negative seawater values. These values are recorded by the precipitation of shell material by certain marine organisms, including brachiopods. Magnitude of evaporative diffusion effect from Koch et al. (1992).

the presence of the SPICE in the nearshore. First, the Laurentian epeiric sea was confined by the carbonate bank and probably not well-circulated. An invading water mass might reach the middle carbonate belt, but would be unlikely to reach the nearshore. Second, if anoxic waters were responsible for faunal mortality, they would need to remain anoxic in the turbulent conditions that prevail above fair-weather wave base.

It seems more likely that the extinction event and the SPICE were driven by increased weathering of the land caused by sea level change (Cowan et al., 2003). Regression exposed large areas of the Laurentian craton for the first time since inundation earlier in the Cambrian. Toxic trace elements (Fig. 10) concentrated in exposed sediments would have been remobilized by rivers and delivered to the epeiric sea. All of the trace elements in Figure 10 are extremely toxic to marine invertebrates (Lussier et al., 1985; Marr et al., 1998). These elements significantly increase mutation rates (Park et al., 1999), oxidize cells in tissues where these elements accumulate (Pedlar et al., 2002), and interfere with a wide variety of physiological processes, including critical metabolic pathways (Bocchetti et al., 2002). One recent study found that increases in copper as low as 6.1 ppm above normal levels can cause significant damage to neural and physiological functions in modern marine invertebrates (Brown et al., 2004). Furthermore, the simultaneous presence of multiple toxins can result in synergistic increases in toxicity (Marr et al., 1998).

Consequently, the influx of lethal trace elements across the Marjumiid-Pterocephaliid biomere boundary had the potential to cause widespread extinction of marine invertebrates. If such a terrigenous flux was indeed responsible for the extinction, the toxic levels should appear earliest—and in the highest concentrations—in the

nearshore. This offers a possible explanation for the observation of Westrop and Ludvigsen (1987) that trilobite families living on the shelf and the upper slope showed higher survivorship across biomere boundaries than families living only on the shelf. It is interesting to note that, while toxic to organisms with developed organ systems, copper has no measureable effect on simple primary producers (Real et al., 2003). If this is true of the other toxic trace elements as well, then such a surge in concentrations would not result in significant impacts on simple primary producers (e.g. phytoplankton).

Accompanying this flux was an increase in concentrations of iron, probably also from the craton. Assuming iron was a limiting nutrient during the Cambrian as it is in the modern, the large influx (Fig. 10) from sea level fall would increase marine primary productivity. As increased production of organic matter exceeded the oxygen available to decompose it, organic (^{13}C -depleted) carbon burial would have increased (Kump and Arthur, 1999; Hartnett and Devol, 2003). The removal of isotopically light ^{12}C from active circulation would increase $\delta^{13}\text{C}$ values throughout the active carbon cycle, resulting in the positive excursion of the SPICE. This provides a possible explanation for why the intensity of the SPICE is inversely correlated with sea level change across the Sauk II-Sauk III boundary.

It is logical to examine why a similar event did not happen during the Sauk I-II subsequence boundary, the other significant regression in the Cambrian. The epeiric sea surrounding Laurentia probably was never more than 150 m deep (Dott and Batten, 1981). Sea level was lower at the time of the Sauk I-Sauk II regression (Fig. 1) and little (if any) of the Laurentian craton was inundated, thus sea level fall at that time would not have exposed large amounts of buried sediments.

Conclusions

This study demonstrates that phosphatic brachiopods offer a valuable chemostratigraphic tool that can be used in Paleozoic siliciclastic rocks. We can conclude:

1. Phosphatic shell material of brachiopods, including those in this study, are capable of preserving isotopic and geochemical information on long time scales ($>500\text{Ma}$).
2. The contribution of isotopically light terrigenous carbon to the total dissolved carbon in the nearshore (20-40%) is responsible for a negative shift in the SPICE relative to micrites from the middle carbonate belt.
3. The relationship between the Sauk II-Sauk III regression, Marjumiid-Pterocephaliid extinction, and the SPICE is consistent with a model in which regression allowed remobilization of previously buried trace elements and Fe resulted in widespread extinction of shelf fauna and an increase in primary productivity, respectively. The latter led to increased organic carbon burial and the carbon isotope excursion of the SPICE.
4. This event was probably unique because it tapped a large reservoir of elements buried in sediments that had been accumulating for much of the Cambrian.

Acknowledgements

This project grew out of work on the Upper Cambrian by Clint Cowan at Carleton College and Tony Runkel at the Minnesota Geological Survey, and both patiently offered indispensable aid. David Fox at the University of Minnesota was also intimately involved with this project. I am indebted to Rick Knurr, who created a new method for running

ICP-MS on biogenic apatites for this study. Sam Matson (University of Minnesota) provided help with the isotopic analyses as well as reviewing this paper. This paper also benefited from critical reviews by Kristin Bergmann and Leah Morgan. I would also like to thank Liz Cassel for explaining that “it’s just comps;” Bereket Haileab, for making me work; my 1994 Subaru for faithfully getting me the University of Minnesota three times a week; and finally the Bernstein Student Research Endowment, for generously funding this project after sending me to Iceland so I could figure out that I didn’t want to do Keck for comps.

References Cited

- Barth, J. A. C., Cronin, A. A., Dunlop, J., and Kalin, R. M., 2003, Influence of carbonates on the riverine carbon cycle in an anthropogenically dominated catchment basin: evidence from major elements and stable carbon isotopes in the Lagan River (N. Ireland): *Chemical Geology*, v. 200, no. 2003, p. 203-216.
- Batts, J. E., Calder, L. J., and Batts, B. D., 2004, Utilizing stable isotope abundances of lichens to monitor environmental change: *Chemical Geology*, v. in press.
- Bocchetti, R., Fattorini, D., Gorbi, S., Machella, N., and Regoli, F., 2002, Unusual bioaccumulation of arsenic in the polychaete *Sabella spallanzanii* and oxidative damages of metals in marine invertebrates: Metal and radionuclides bioaccumulation in marine organisms, CIESM Workshop Monograph #19, p. 85-87.
- Brasier, M. D., 1993, Towards a carbon isotope stratigraphy of the Cambrian system: Potential of the Great Basin succession, in Hailwood, E. A., and Kidd, R. B., eds., *High resolution stratigraphy*, Geological Society (London), p. 341-350.
- Brasier, M. D., and Sukhov, S. S., 1998, The falling amplitude of carbon isotope oscillations through the Lower to Middle Cambrian: Northern Siberia data: *Canadian Journal of Earth Sciences*, v. 35, no. 4, p. 353-373.
- Brown, R. J., Galloway, T. S., Lowe, D., Browne, M. A., Dissanayake, A., Jones, M. B., and Depledge, M. H., 2004, Differential sensitivity of three marine invertebrates to copper assessed using multiple biomarkers: *Aquatic Toxicology*, v. 66, no. 3, p. 267-278.
- Chao, Y., Telmer, K., and Veizer, J., 1996, Chemical dynamics of the "St. Lawrence" riverine system: δD_{H_2O} , $\delta^{18}O_{H_2O}$, $\delta^{13}C_{DIC}$, $\delta^{34}S_{sulfate}$, and dissolved $^{87}Sr/^{86}Sr$: *Geochimica et Cosmochimica Acta*, v. 60, no. 5, p. 851-866.

- Cowan, C. A., Runkel, A. C., and Saltzman, M. R., 2003, Presentation: The effect on paleo-productivity of the first major delivery of mid-Laurentian saprolite-derived material to Phanerozoic oceans: Continent-wide marine ravinement during submergence-emergence of the Late Cambrian North America, and the global carbon isotope SPICE event, GSA Annual Meeting: Seattle, Geologic Society of America.
- Dott, R. H., 2003, The importance of eolian abrasion in supermature quartz sandstones and the paradox of weathering on vegetation-free landscapes: *Journal of Geology*, v. 111, no. 4, p. 387-405.
- Dott, R. H., and Batten, R. L., 1981, *Evolution of the Earth*: New York, McGraw-Hill, 573 p.
- Elderfield, H., Upstill-Goddard, R., and Sholkovitz, E. R., 1990, The rare earth elements in rivers, estuaries, and coastal seas and their significance to the composition of ocean waters: *Geochimica et Cosmochimica Acta*, v. 54, p. 971-991.
- Glumac, B., and Walker, K. R., 1998, A Late Cambrian positive carbon-isotope excursion in the southern Appalachians: Relation to biostratigraphy, sequence stratigraphy, environments of deposition, and diagenesis: *Journal of Sedimentary Research*, v. 68, p. 1212-1222.
- Halley, R. B., and Roullet, L. M., 1999, Reconstruction the history of Eastern and Central Florida Bay using mollusk-shell isotope records: *Estuaries*, v. 22, no. 2B, p. 358-368.
- Hartnett, H. E., and Devol, A. H., 2003, Role of a strong oxygen-deficient zone in the preservation and degradation of organic matter: A carbon budget for the continental margins of northwest Mexico and Washington State: *Geochimica et Cosmochimica Acta*, v. 67, no. 2, p. 247-264.
- Holser, W. T., 1997, Evaluation of the application of rare-earth elements to paleoceanography: *Palaeogeography, Palaeoclimatology, Palaeoecology*, v. 132, no. 1997, p. 309-323.
- Koch, P. L., Zachos, J. C., and Gingerich, P. D., 1992, Correlation between isotope records in marine and continental carbon reservoirs near the Palaeocene/Eocene boundary: *Nature*, v. 358, p. 319-322.
- Kump, L. R., and Arthur, M. A., 1999, Interpreting carbon-isotope excursions: carbonates and organic matter: *Chemical Geology*, v. 161, no. 1999, p. 181-198.
- Laenen, B., Hertogen, J., and Vandenberghe, N., 1997, The variation of the trace-element content of fossil biogenic apatite through eustatic sea-level cycles: *Palaeogeography, Palaeoclimatology, Palaeoecology*, v. 132, no. 1997, p. 325-342.
- Latham, M., 1975, Soils of an ultramafic complex from the western coast of New Caledonia; Boulinda; I. Generalities, distribution of soils in the complex, and humic accumulation soils: *Cahiers O.R.S.T.O.M.: Pedologie*, v. 31, no. 1, p. 27-40.
- Lécuyer, C., Grandjean, P., Barrat, J.-A., Nolvak, J., Emig, C. C., Paris, F., and Robardet, M., 1998, $\delta^{18}\text{O}$ and REE contents of phosphatic brachiopods: A comparison

- between modern and lower Paleozoic populations: *Geochimica et Cosmochimica Acta*, v. 62, no. 14, p. 2429-2436.
- Lécuyer, C., Grandjean, P., and Emig, C. C., 1996, Determination of oxygen isotope fractionation between water and phosphate from living lingulids: Potential application to palaeoenvironmental studies: *Palaeogeography, Palaeoclimatology, Palaeoecology*, v. 126, no. 1996, p. 101-108.
- Lécuyer, C., Reynard, B., and Grandjean, P., 2004, Rare earth element evolution of Phanerozoic seawater recorded in biogenic apatites: *Chemical Geology*, v. 204, no. 2004, p. 63-102.
- Lee, X., and Wan, G., 2000, No vital effect on $\delta^{18}\text{O}$ and $\delta^{13}\text{C}$ values of fossil brachiopod shells, Middle Devonian of China: *Geochimica et Cosmochimica Acta*, v. 64, no. 15, p. 2649-2664.
- Levin, H. L., 1999, *Ancient Invertebrates and Their Living Relatives*: Upper Saddle River, NJ, Prentice Hall, 358 p.
- Lussier, S. M., Gentile, J. H., and Walker, J., 1985, Acute and chronic effects of heavy metals and cyanide on *Mysidopsis bahia*: *Aquatic Toxicology*, v. 7, no. 1-2, p. 25-35.
- Marr, J. C. A., Hansen, J. A., Meyer, J. S., Cacela, D., Podrabsky, T., Lipton, J., and Bergman, H. L., 1998, Toxicity of cobalt and copper to rainbow trout: application of a mechanistic model for predicting survival: *Aquatic toxicology*, v. 43, no. 4, p. 225-238.
- McLennan, S. M., 1989, Rare earth elements in sedimentary rocks: Influence of provenance and sedimentary processes, *Reviews in Mineralogy* 21, p. 169-200.
- Montañez, I. P., Banner, J. L., Osleger, D. A., Borg, L. E., and Bosserman, P. J., 1996, Integrated Sr isotope variations and sea-level history of Middle to Upper Cambrian platform carbonates: Implications for the evolution of Cambrian seawater $^{87}\text{Sr}/^{86}\text{Sr}$: *Geology*, v. 24, no. 10, p. 917-920.
- Montañez, I. P., Osleger, D. A., Banner, J. L., Mack, L. E., and Musgrove, M., 2000, Evolution of the Sr and C isotope composition of Cambrian Oceans: *GSA Today*, v. 10, no. 5.
- Palmer, A. R., 1965, Biome-A new kind of biostratigraphic unit: *Journal of Paleontology*, v. 39, p. 149-153.
- , 1971, The Cambrian of the Great Basin and Adjacent Areas, in Holland, C. H., ed., *Cambrian of the New World*: New York, Wiley-Interscience, p. 1-78.
- , 1981, Subdivision of the Sauk Sequence, in Taylor, M. E., ed., *Short papers for the second international symposium on the Cambrian System*: U.S. Geological Survey Open-File Report 81-743, p. 160-162.
- , 1984, The biome problem: Evolution of an idea: *Journal of Paleontology*, v. 58, no. 3, p. 599-611.
- , 1998, A proposed nomenclature for stages and series for the Cambrian of Laurentia: *Canadian Journal of Earth Sciences*, v. 35, no. 4, p. 323-328.

- Park, K. S., Song, J.-I., Choe, B. L., and Kim, S. J., 1999, Amylase polymorphism of *Littorina brevicula* from polluted and unpolluted sites, Korea: Bulletin of Environmental Contamination Toxicology, v. 63, p. 633-638.
- Pedlar, R. M., Ptashynski, M. D., Evans, R., and Klaverkamp, J. F., 2002, Toxicological effects of dietary arsenic exposure in lake whitefish (*Coregonus clupeaformis*): Aquatic Toxicology, v. 57, no. 3, p. 167-189.
- Perfetta, P. J., Shelton, K. L., and Stitt, J. H., 1999, Carbon isotope evidence for deep-water invasion at the Marjumiid-Pteroccephaliid biomere boundary, Black Hills, USA: A common origin for biotic crises on Late Cambrian shelves: Geology, v. 27, no. 5, p. 403-406.
- Picard, S., Lécuyer, C., Barrat, J.-A., Garcia, J.-P., Dromart, G., and Sheppard, S. M. F., 2002, Rare earth element contents of Jurassic fish and reptile teeth and their potential relation to seawater composition (Anglo-Paris Basin, France and England): Chemical Geology, v. 186, no. 2002, p. 1-16.
- Real, M., Muñoz, I., Guasch, H., Navarro, E., and Sabater, S., 2003, The effect of copper exposure on a simple aquatic food chain: Aquatic Toxicology, v. 63, no. 3, p. 283-291.
- Reynard, B., Lécuyer, C., and Grandjean, P., 1999, Crystal-chemical controls on rare-earth element concentrations in fossil biogenic apatites and implications for paleoenvironmental reconstructions: Chemical Geology, v. 155, no. 1999, p. 233-241.
- Rodland, D. L., Kowalewski, M., Dettman, D. L., Flessa, K. W., Atudorei, V., and Sharp, Z. D., 2003, High-resolution analysis of $\delta^{18}\text{O}$ in the biogenic phosphate of modern and fossil lingulid brachiopods: Journal of Geology, v. 111, p. 441-453.
- Rollinson, H., 1993, Using Geochemical Data: Evaluation, Presentation, Interpretation: London, Prentice-Hall, 352 p.
- Runkel, A. C., McKay, R. M., and Palmer, A. R., 1998, Origin of a classic cratonic sheet sandstone: Stratigraphy across the Sauk II-Sauk III boundary in the Upper Mississippi Valley: GSA Bulletin, v. 110, no. 2, p. 188-210.
- Saltzman, M. R., Cowan, C. A., Runkel, A. C., Runnegar, B., and Denniston, R., 2004, The Upper Cambrian SPICE ($\delta^{13}\text{C}$) event and the Sauk II-Sauk III regression: New evidence from Laurentian basins in Utah, Iowa, and Newfoundland: Journal of Sedimentary Research, v. in press.
- Saltzman, M. R., Davidson, J. P., Holden, P., Runnegar, B., and Lohmann, K. C., 1995, Sea-level-driven changes in ocean chemistry at an Upper Cambrian extinction horizon: Geology, v. 23, no. 10, p. 893-896.
- Saltzman, M. R., Ripperdan, R. L., Brasier, M. D., Lohmann, K. C., Robison, R. A., Chang, W. T., Peng, S., Ergaliev, E. K., and Runnegar, B., 2000, A global carbon isotope excursion (SPICE) during the Late Cambrian: Relation to trilobite extinctions, organic-matter burial and sea level: Palaeogeography, Palaeoclimatology, Palaeoecology, v. 162, no. 2000, p. 211-223.
- Saltzman, M. R., Runnegar, B., and Lohmann, K. C., 1998, Carbon isotope stratigraphy of Upper Cambrian (Steptoean Stage) sequences of the eastern Great Basin: Record of a global oceanographic event: GSA Bulletin, v. 110, no. 3, p. 285-297.

- Sarkar, A., Bhattacharya, S. K., and Chakrabarti, A., 2003, Presentation: Stable isotopes of estuarine water and oyster shells from Ganges Delta, India: Paleoenvironmental implications, INQUA Congress: Reno, Geological Society of America.
- Stearn, C. W., and Carroll, R. L., 1989, *Paleontology: The Record of Life*: New York, John Wiley & Sons, 453 p.
- Telmer, K., and Veizer, J., 1999, Carbon fluxes, $p\text{CO}_2$ and substrate weathering in a large northern river basin, Canada: carbon isotope perspectives: *Chemical Geology*, v. 159, no. 1999, p. 61-86.
- Thomas, R. C., 1993, The Marjumiid-Pterocephaliid (Upper Cambrian) mass extinction event in the western United States [Ph.D. thesis]: University of Washington, 352 p.
- Walker, R. G., and Plint, A. G., 1992, Wave- and storm-dominated shallow marine settings, in Walker, R. G., and James, N. P., eds., *Facies Models: Response To Sea Level Change*, Geological Association of Canada, p. 219-238.
- Westrop, S. R., and Ludvigsen, R., 1987, Biogeographic control of trilobite mass extinction at an Upper Cambrian "biomere" boundary: *Paleobiology*, v. 13, no. 1, p. 84-99.
- Williams, A., and Cusack, M., 1999, Evolution of a rhythmic lamination in the organophosphatic shells of brachiopods: *Journal of Structural Biology*, v. 126, p. 227-240.
- Williams, A., Cusack, M., and MacKay, S., 1994, Collagenous chitinophosphatic shell of the brachiopod *Lingula*: *Philosophical Transactions of the Royal Society of London, Series B*, v. 346, p. 223-266.
- Wright, J., Schrader, H., and Holser, W. T., 1987, Paleoredox variations in ancient oceans recorded by rare earth elements in fossil apatite: *Geochimica et Cosmochimica Acta*, v. 51, p. 631-644.

Appendix 1

	Hudson	BC-1	BC-1	BC-1	AC-1	AC-1	BC-1	BC-1	BC-1	BC-1	BC-1	BC-1	BC-1
	2 703'7"	707'11"	745'10"	736'0"	736'10"	802'1"	859'6"	860'9.5"	860'9.5"	860'9.5"	860'9.5"	864'1"	865'6"
²³ Na	8941	7833	8132	5108.5	7763.5	11335	3299	6446	6023	5960.5	6072.5	5921	6183.5
²⁶ Mg	2381	2684	1934	2260	2343.5	2166	12810	2052	1853	1845	1829.5	1601.5	2123
²⁷ Al	1338.5	573.4	2272	990.5	939.6	204.1	1792.5	414.4	343	340.2	292.6	1158	265.1
²⁹ Si	3155	469.5	2779.5	219	176.1	71.2	5732.5	496	538.6	541.9	232.1	2013.5	762.4
³¹ P	146750	157250	139450	142750	146400	135400	134000	153850	151950	152350	152850	151050	157450
³⁹ K	1367.5	383.5	1535	417	306	216	2505.5	477.5	392	340	277	997.5	234
⁴⁴ Ca	374600	402750	338800	346550	354750	343150	379500	396800	389400	390950	387550	387700	395250
⁵⁴ Fe	10013.5	7326	46125	46525	44180	45805	10490	3787.5	4021.5	3965.5	3978.5	9627	4469.5
⁵⁵ Mn	638.1	881.7	2450.5	1428.5	930.3	1237.5	1306	4698.5	4688.5	4660	4652	4114	5260.5
⁷ Li	3.84	4.79	3.64	3.61	5.08	4.05	1.41	2.88	2.75	2.6	2.5	2.5	3.19
¹¹ B	46.39	59.08	32.21	42.98	38.57	54.38	51.1	89.16	95	94.33	77.44	71.42	103.4
²⁷ Al	1685	612.8	2640	1087	1164	220.8	2094	530.7	415.7	444.7	358	1321	334.1
⁴⁷ Ti	284	238.9	227.9	215.5	244.4	217.3	251.5	251.2	256.1	282.6	268.5	474.2	273.9
⁵² Cr	8.56	1.58	5.26	3.39	4.28	3.16	4.88	3.47	3.32	3.45	3.28	72.76	3.08
⁵⁹ Co	2.19	77.63	203.8	78.41	333.8	382.4	5.19	1.36	0.7	0.79	0.77	5.52	0.67
⁶⁰ Ni	22.68	65.23	202.3	169.6	247	227.8	19.96	9.18	10.42	10.83	10.45	20.56	6.98
⁶⁵ Cu	297.7	301	445.5	181.5	257.2	510.1	109.2	79.46	92.34	114.2	94.31	466.6	257.5
⁶⁶ Zn	1081	532.8	596.2	35.24	476.9	798.4	139.5	120.9	186.9	196.9	192.4	251.1	153
⁷⁵ As	24.66	61.3	135.3	56.05	166.8	171.2	14.21	18.16	16.46	18.91	16.74	24.55	19.56
⁸² Se	224.3	102.9	65.22	61.24	265	0	58.08	158.7	69.08	77.66	72.84	199.5	80.41
⁸⁵ Rb	3.09	0.99	4.38	1.59	1	0.77	6.2	0.96	1.03	1.04	0.83	1.94	0.76
⁸⁸ Sr	3409.5	4380	4127	4432.5	4007.5	4091.5	1396.5	4556	4421.5	4450.5	4485.5	3846.5	4729.5
⁸⁹ Y	568.9	575.9	551.1	637.1	589.9	503.5	290.4	679.8	673	673.8	675.7	621.2	627.9
⁹⁸ Mo	1.97	3.38	6.44	5.96	9.85	11.7	2.23	1.22	2.56	2.13	1.46	3.21	1.09
¹¹⁴ Cd	3.19	0.54	0.61	0.41	0.16	0.23	0.08	0.15	0.13	0.14	0.11	0.13	0.11
¹³³ Cs	0.09	0.11	0.13	0.13	0.08	0.11	0.29	0.11	0.12	0.07	0.05	0.15	0.05
¹³⁸ Ba	233.95	371.1	345.05	217	376.4	350.8	168.5	453.4	451.2	459.55	460.9	355	441.15
¹⁸² W	1.79	2.87	1.95	1.51	1.1	2.82	3.85	1.06	4.08	2.02	1.32	1.78	2.37
²⁰⁵ Tl	0.36	1.12	3	2.06	2.37	3.43	0.83	0.1	0.87	0.29	0.14	0.24	0.27
²⁰⁸ Pb	160.6	55.83	184.4	136.6	175.3	189.3	8.01	26.35	30.14	33.06	30.2	66.98	36.79
²³² Th	10.07	31.14	13.2	11.17	38.38	34.85	7.68	107.7	80.87	81.66	80.87	33.32	86.06
²³⁸ U	31.01	29.01	32.64	13.1	42.45	35.26	28.21	40.1	42.77	44.1	43.72	52.38	33.56
¹³⁹ La	887.6	706.6	875.3	894.3	655.2	581.1	454.8	808.3	753.4	753.9	758.3	792.1	827.8
¹⁴⁰ Ce	5563	4403	5387	4999	4121	3495	2350	6518	4533	4698	4858	6107	4963
¹⁴¹ Pr	342.4	282.6	370.1	362.9	272.5	237.7	178.7	372.5	337.5	338.6	341.3	359.8	403.3
¹⁴⁶ Nd	1446	1258	1645	1650	1222	1070	717.6	1612	1469	1478	1478	1608	1854
¹⁴⁷ Sm	291.8	273.3	349.2	369.9	266.7	235.1	127.7	336.6	317.3	318.1	317.8	350.3	426.4
¹⁵¹ Eu	70.45	64.3	80.64	86.29	59.38	54.29	30.44	72	70.36	70.27	70.16	79.06	97.14
¹⁵⁷ Gd	260.9	248.6	293	326.1	238.2	211	112.9	293.1	283.5	284.9	286	301.6	359.8
¹⁵⁹ Tb	33	31.44	35.55	41.01	30.38	26.66	13.28	37.57	37.47	37.12	37.26	36.94	43.57
¹⁶³ Dy	146.6	138.4	148	171.6	137.1	116.6	57.99	170.1	169.5	169.3	169.9	158.3	178
¹⁶⁵ Ho	23	22.44	22.81	26.26	22.39	18.93	10.1	27.96	27.95	28.05	28.04	24.94	26.56
¹⁶⁶ Er	50.52	49.1	48.55	54.71	50.09	42.37	23.77	61.86	61.43	62.27	62.2	54.85	54.04
¹⁶⁹ Tm	5.32	5.11	4.82	5.26	5.37	4.57	2.77	6.28	6.31	6.33	6.28	5.54	4.88
¹⁷² Yb	26.27	24.32	22.68	23.88	25.81	22.68	15.13	29.3	28.55	28.75	28.56	27.58	21.12
¹⁷⁵ Lu	3.46	3.37	3.05	3	3.46	3.18	2.42	3.74	3.72	3.65	3.62	3.59	2.56

Figure A1. Major, trace, and rare earth abundances in phosphatic brachiopod shells. All concentrations are given in ppm. Na and K concentrations are taken from ion chromatography results, which gave highly similar results with higher detection limits.